



Cite this: RSC Adv., 2016, 6, 507

Titanium aminophosphates: synthesis, characterization and crystal violet dye degradation studies†

Rajini Anumula, Ajay Kumar Adepu, Suman Chirra, Suresh Siliveri and Venkatathri Narayanan*

Titanium aminophosphates are prepared by using titanium tetraisopropoxide, orthophosphoric acid and aliphatic amines. The synthesized titanium *n*-propylaminophosphate (TNPAP), titanium *n*-octylaminophosphate (TNOAP) and titanium *n*-dodecylaminophosphate (TNDDAP) are characterized by various physicochemical techniques. The powder X-ray diffraction pattern of titanium aminophosphates suggests the presence of a $-Ti-O-$ phase. The percentage of titanium incorporated ($P/Ti = 100$) into the frameworks of the titanium aminophosphates have been confirmed from EDAX analysis. The infrared and Raman spectra infer the presence of peaks due to the vibrational bands of $Ti-O$, $P-O$ and $Ti-O-P$ linkages. The Ultraviolet-Visible diffuse reflectance spectra reveal the presence of tetrahedral co-ordination of Ti in the framework. The X-ray photoelectron spectra suggest the presence of an $-O-Ti-N-$ or $-Ti-N-O-$ framework in TNPAP. The ^{31}P MASNMR spectra of titanium aminophosphates indicate the presence of tetrahedrally co-ordinated phosphorous in the framework. The catalytic effect of TNPAP, TNOAP and TNDDAP has been studied for the degradation of crystal violet dye. TNPAP has been found to be more efficient for the degradation of crystal violet, indicating the specificity of this catalyst. The optimum conditions required for the efficient degradation of crystal violet dye have been established as $pH = 5.1$, $[H_2O_2] = 1.0 \times 10^{-3}$ M, $[CV] = 8.0 \times 10^{-4}$ M and TNPAP catalyst dosage of 150 mg. About 91% of the crystal violet dye has been degraded by TNPAP in 165 min. These catalysts exhibited good reusability over five successive cycles. They have the potential to be used as economical catalysts for dye degradation of industrial waste waters.

Received 23rd October 2015
Accepted 2nd December 2015

DOI: 10.1039/c5ra22210a
www.rsc.org/advances

Introduction

Organic dyes are major pollutants released into water systems during their manufacturing and processing from industry. These compounds are highly coloured and cause serious problems to the aquatic environment as they affect the photosynthetic activity by reducing light penetration. Their presence in as low concentration as 1 mg L^{-1} in the effluent is considered undesirable and needs to be removed before the wastewater can be discharged into the environment.¹ In addition, their presence in drinking water constitutes a potential human health hazard. They are difficult to degrade due to their complex structures, which makes them mutagenic and carcinogenic. Thus, efficient colour removal from wastewaters involving physical, chemical and biological methods has attracted the interest of environmentalists and researchers. The majority of the dyes consumed at the industrial scale have azo,

anthraquinone, triphenylmethane, phthalocyanine, formazin or oxazine functional groups.² These dyes are used extensively in textile industries owing to their brilliant colour, high wetfastness, easy application and minimum requirement of energy consumption during processing.

Triphenylmethane dyes are aromatic xenobiotic compounds used extensively in dye stuff manufacturing industries, as biological stains, dermatological agents and in textile printing. These dye effluents pose a major threat to the ecosystem. Crystal violet (CV) (Fig. 1) belongs to the class of triphenylmethane dyes and is used as a DNA label.³ This dye is non-biodegradable, toxic, mutagenic and a mitotic poison.⁴

Synthetic dyes are recalcitrant to removal by conventional wastewater treatment technologies such as adsorption, photo-degradation, coagulation, flocculation, chemical oxidation, electrochemical oxidation and biological processing. Available physical and chemical treatment methods have limited use and are operationally expensive. Research efforts are needed to develop powerful techniques for the removal of triphenylmethane dyes from the aqueous medium to avoid their accumulation in the environment. Therefore, there is a need for efficient water treatment technologies to degrade hazardous

Department of Chemistry, National Institute of Technology, Warangal 506 004, Telangana, India. E-mail: venkatathrin@yahoo.com; Tel: +91-9491319976

† Electronic supplementary information (ESI) available. See DOI: [10.1039/c5ra22210a](https://doi.org/10.1039/c5ra22210a)

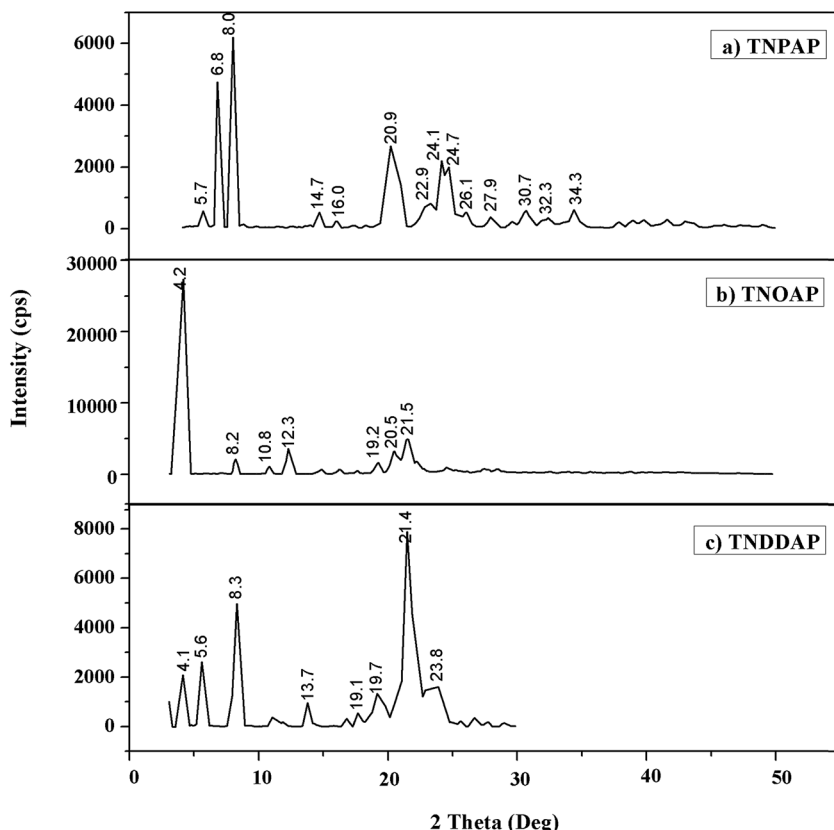


Fig. 1 Powder XRD patterns of (a) TNPAP, (b) TNOAP and (c) TNDDAP.

contaminants present in the effluents and make water resources both safe and potable.

Phosphate based materials are important in several industrial acid catalysed reactions.⁵ In recent years, inorganic phosphorous containing materials have received much attention on account of their ability to selectively uptake specific ions, resistance to oxidation, high thermal stability and high chemical stability. In addition, the presence of phosphate in materials seems to enhance catalytic properties, stabilize surface areas, stabilize crystal phases, improve surface acidity and make the materials porous.⁶ Research on phosphate based materials with open frameworks is currently in progress due to their applications in catalysis and gas separation.⁷ The study of phosphates of transition metals has received great attention in recent years. Phosphate frameworks stabilize reduced oxidation states, due to its high charge (PO_4^{3-}) and therefore favour the formation of anionic frameworks with a high degree of chemical, mechanical and thermal stability.

Aminophosphates are a novel group of materials. The organic functionality in the aminophosphate framework enhances hydrophobicity and shows high activity in base catalyzed reactions. Incorporation of transition metals, such as titanium or vanadium or palladium, in aminophosphates leads to novel materials with redox properties. In particular, the titanium cation Ti^{4+} in framework positions is found to exhibit good activity in shape-selective redox reactions.⁸

This manuscript deals with the synthesis, detailed characterization and catalytic crystal violet dye degradation studies of titanium aminophosphates. Owing to the presence of titanium that has redox, Lewis acid, Bronsted acid sites as well as Lewis base nitrogen donor alkyl groups, the materials are expected to have peculiar catalytic applications. Titanium aminophosphates have been investigated for their catalytic applications towards the degradation of crystal violet dyes at room temperature using hydrogen peroxide as the oxidant.

Experimental

Synthesis of titanium aminophosphates was carried out at room temperature. In a typical synthesis, *n*-propyl amine (10.9 mL) or *n*-octyl amine (22.0 mL) or *n*-dodecyl amine (30.6 mL) was added to 0.05 mL of titanium tetraisopropoxide and was stirred. To this mixture, 1.87 mL of orthophosphoric acid was added and stirred vigorously to yield solid products ($0.02\text{TiO}_2 : \text{P}_2\text{O}_5 : 8\text{RNH}_2$). The products thus obtained were thoroughly washed with ether, dried at 40 °C for about 30 min and ground to fine powder to obtain the respective titanium aminophosphates.

Qualitative phase analysis of titanium aminophosphates have been studied using a Bruker AXS D8 Advance diffractometer at room temperature with $\text{Cu-K}\alpha$ X-ray source of wavelength 1.5406 Å using a Si (Li) PSD detector. The morphology and surface elemental composition of the material was investigated using scanning electron microscopy (SEM/EDAX) on a JEOL

Model JSM-6390LV. Fourier transform infrared (FT-IR) spectroscopy was obtained on a Thermo Nicolet, Avatar 370 spectrophotometer equipped with a pyroelectric detector (DTGS type); a resolution of 4 cm^{-1} was adopted and provided with a KBr beam splitter. Dispersive Raman spectroscopy was performed on a Bruker Senterra at a wavelength of 532 nm using laser radiation as the source. The co-ordination and oxidation state of titanium was examined by diffuse reflectance UV-Visible spectrophotometer (UV-Vis DRS) on a Varian, Cary 5000 in the wavelength range of 175–800 nm. X-ray photoelectron spectroscopic analysis was carried out using ESCA-3000 (VG Scientific, UK) instrument. The ^{31}P magic-angle spinning (MAS) nuclear magnetic resonance (NMR) spectroscopy was performed at room temperature on a Bruker DRX-500 AV-III 500(S) spectrometer, with a spinning rate of 10–12 kHz operating at 121.49 MHz using a 5 mm dual probe. ^{13}C cross polarization magic-angle spinning (CP-MAS) nuclear magnetic resonance (NMR) spectroscopy was performed at room temperature on a DSX-300 Avance-III 400(L) NMR spectrometer with a spinning rate of 10–12 kHz operating at 75.47 MHz using a 5 mm dual probe.

The degradation of crystal violet dye using hydrogen peroxide as the oxidant in presence of titanium aminophosphates has been studied at room temperature. A stock solution of dye having a concentration of $1 \times 10^{-3}\text{ M}$ was prepared and solutions of desired concentrations have been obtained by the successive dilutions of stock solution. The degradation has been studied using an Ultraviolet-Visible spectrophotometer by measuring the decrease in absorbance of the dye solution with respect to time at the λ_{max} of dye, *i.e.* 580 nm for crystal violet. The effect of pH, concentration of the dye, concentration of oxidant H_2O_2 and amount of catalyst on the degradation has been studied. All the studies were carried out under room temperature conditions.

Results and discussion

Powder X-ray diffraction patterns of titanium *n*-propylaminophosphate, titanium *n*-octylaminophosphate and titanium *n*-dodecylaminophosphate are shown in Fig. 1. TNPAP exhibits peaks at 2θ degrees of 22.9° , 24.1° , 26.1° , 27.9° and 30.7° indicates the presence of $-\text{Ti}-\text{O}-$ linkage.⁹ Similarly, X-ray diffraction pattern of TNOAP and TNDDAP shows peaks at 2θ degrees of 5.6° , 8.2° , 8.3° , 13.7° and 18.7° corresponding to the presence of $-\text{Ti}-\text{O}-$ with a mesoporous structure.^{9–11} TNOAP and TNDDAP exhibit low angle diffraction peaks at 4.1° and 4.2° , respectively, characteristic of a mesoporous structure.

The SEM-EDAX images of TNPAP, TNOAP and TNDDAP are shown in Fig. 2. The SEM images of TNPAP, TNOAP and TNDDAP reveal that the materials possess micron sized irregular flakes throughout the surface of the materials. The EDAX analysis of TNPAP, TNOAP and TNDDAP show the distribution of the constituent elements O, C, N, P, and Ti.

The thermogravimetry/differential thermal analysis of TNPAP, TNOAP and TNDDAP show continuous weight loss up to $400\text{ }^\circ\text{C}$. This may be due to removal of polymerized molecules. Thereafter, the weight remains constant, which indicates

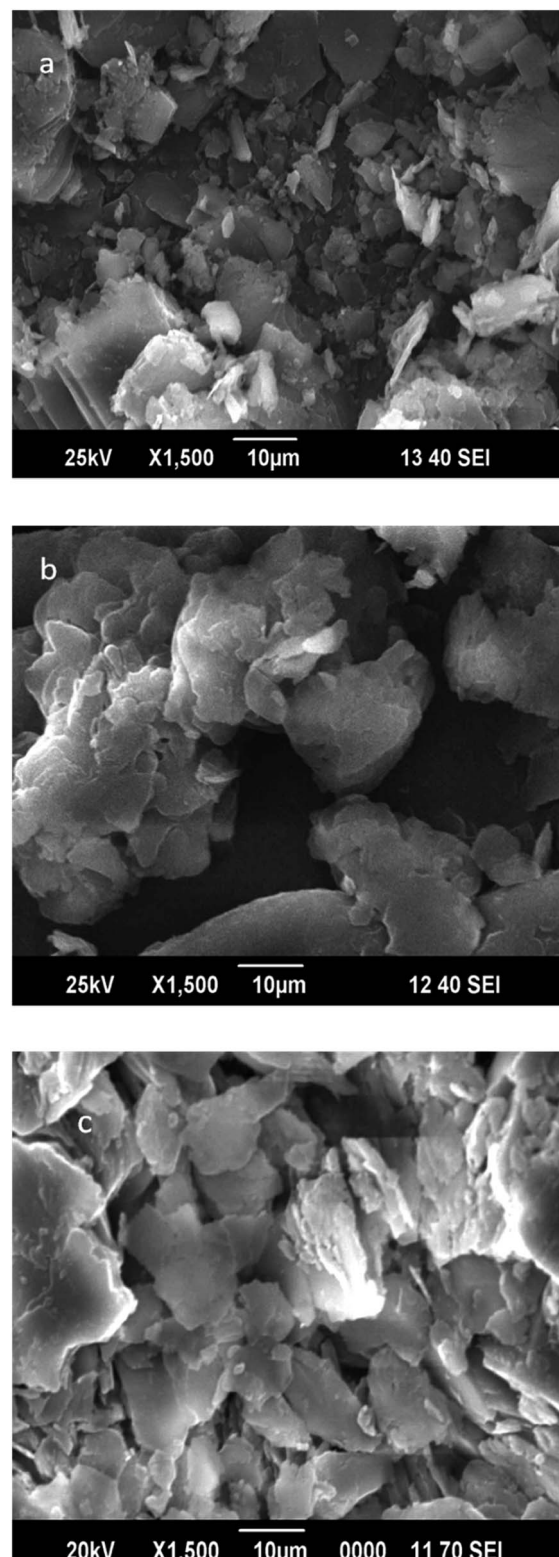


Fig. 2 SEM images of (a) TNPAP, (b) TNOAP and (c) TNDDAP.

the decomposition, combustion and crystallization of organic material present in titanium aminophosphates. DTA shows endothermic peaks due to dehydration and evaporation of

organic components followed by exothermic peaks due to the oxidative decomposition of the template.

The BET surface area analysis of titanium aminophosphates show 60, 80 and 100 $\text{m}^2 \text{ g}^{-1}$ of surface area for TNPAP, TNOAP and TNDDAP, respectively. The lesser surface areas compared to those reported for zeolites is due to the blockage of pores by alkyl groups present in the amines.

The FT-IR spectra of TNPAP, TNOAP and TNDDAP show broad absorption bands at 3420 cm^{-1} , which correspond to O-H or N-H stretching vibrations. The peaks in the range of $3020\text{--}2850 \text{ cm}^{-1}$ correspond to the alkyl symmetrical and asymmetric stretching vibrations of amine groups in titanium aminophosphates.¹² Peaks in the range of $1640\text{--}1630 \text{ cm}^{-1}$ are attributed to O-H bending vibrations of adsorbed water in titanium aminophosphates. Peaks observed at 1469 and 1467 cm^{-1} are due to asymmetric deformation vibrations of the alkyl group in TNOAP and TNDDAP.¹³ The bands at 1079 and 1085 cm^{-1} in TNOAP and TNDDAP are attributed to P-O stretching vibrations.^{14,15} The bands at 1038 and 1034 cm^{-1} in TNPAP and TNOAP are due to Ti-O-P stretching vibrations. The bands around 980 cm^{-1} are attributed to vibrational frequencies of the P-O groups in the titanium aminophosphates.¹⁵ Peaks at 1240 and 1222 cm^{-1} in TNOAP and TNDDAP correspond to the characteristic absorbance of C-N bonds.¹⁶ The peaks at 887 and 892 cm^{-1} in TNOAP and TNDDAP are due to the asymmetric stretching vibrations of P-O-P groups. The peaks at 759 and 758 cm^{-1} in TNPAP and TNOAP are attributed to non-bridging Ti-O bond vibrations.^{17,18} The peaks at about 725 and 723 cm^{-1} in TNOAP and TNDDAP are assigned to symmetric stretching vibrations of P-O-P groups. The peaks in the range of $700\text{--}400 \text{ cm}^{-1}$ are attributed to Ti-O and Ti-O-Ti vibrations in titanium aminophosphates. The peaks at 538, 492, 530 and 540 cm^{-1} in titanium aminophosphates are attributed to P-O bending vibrations.^{19,20}

The Raman spectra of TNPAP, TNOAP and TNDDAP show small peaks at 568 cm^{-1} and 939 cm^{-1} and correspond to the stretching vibration of the Ti-O bond.^{21,22} The band at 1200 cm^{-1} in TNPAP is associated with the asymmetric stretching vibration of the P-O bond in phosphate groups.²³

The UV-Visible diffuse reflectance spectra of TNPAP, TNOAP and TNDDAP show a peak around 215 nm due to charge transfer transitions between empty 3d-orbital's of Ti(IV) cations and 2p-orbitals of oxygen anions (O^{2-}). The charge transfer transition infers the presence of titanium in tetrahedral coordination. TNPAP, TNOAP and TNDDAP show peaks at 343, 330 and 325 nm, respectively. These can be attributed to the existence of titanium in a tetrahedral coordination.

The X-ray photo electron (XPS) spectra of carbon, oxygen, nitrogen, phosphorous and titanium ions show the carbon 1s peak at 288.0 eV. This can be attributed to carbon bonded to oxygen, nitrogen and hydrogen.²⁴ The peak around 534.0 eV corresponds to the oxygen 1s binding energy. This is due to chemisorbed water and weakly adsorbed oxygen molecules on the surface. The binding energies of 534.2 eV and 532.4 eV are ascribed to oxygen co-contributed from Ti-O, P-O.²⁵ The peaks at 462 and 468 eV correspond to the binding energies of Ti 2p_{3/2} and 2p_{1/2} electrons, which is due to nitrogen doped interstitially into the titanium matrix.²² The higher binding energy value of titanium is due to the different electronic interactions with nitrogen compared to oxygen. They suggest considerable modification of the lattice due to N substitution. Titanium binds to nitrogen or oxygen atoms in the lattice to form O-Ti-N or Ti-N-O.²⁶ The P 2p shows a peak at 136.0 eV corresponding to the presence of phosphorous oxide (P_2O_5) in the TNPAP.²³

The ³¹P MASNMR spectra of TNPAP, TNOAP and TNDDAP are shown in Fig. 3. TNPAP shows peaks at 4.654 ppm and -0.73 ppm with its side bands. The peaks are in 1 : 3 intensity ratios and suggest the existence of two crystallographically non-equivalent phosphorous atoms. The ³¹P MASNMR spectra of TNOAP and TNDDAP show peaks at 5.824 and 1.924 ppm. The presence of only one peak in TNOAP and TNDDAP spectra indicates that there is a unique chemical environment for the phosphorous atoms. The ³¹P peaks in the range of -5 to 3 ppm correspond to the presence of a mesoporous crystalline titanium phosphate framework in the titanium aminophosphates.²⁷

The ¹³C MASNMR spectra of TNPAP, TNOAP and TNDDAP show peaks at 41.12 and 39.80 ppm, which corresponds to the C₁, carbon bonded to the nitrogen atom of the amine group.

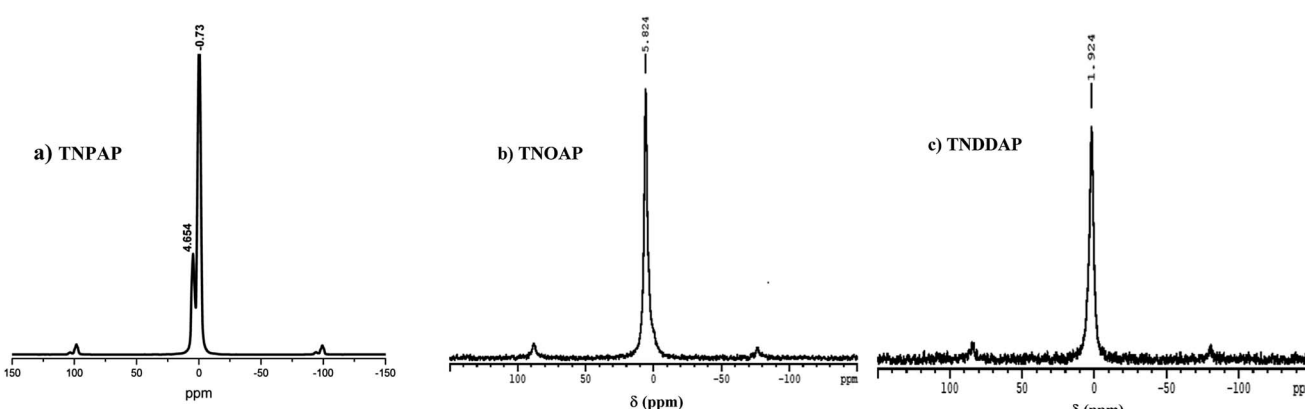


Fig. 3 ³¹P MASNMR spectra of (a) TNPAP, (b) TNOAP and (c) TNDDAP.

Table 1 Effect of pH on the degradation of crystal violet^a

pH	% degradation		
	TNPAP	TNOAP	TNDDAP
2.7	64.1	61.2	67.3
3.1	78.2	75.2	71.8
5.1	91.4	79.0	81.8

^a [CV] = 8.0 × 10⁻⁴ M, [H₂O₂] = 1.0 × 10⁻³ M, pH = 5.1, catalyst dosage = 150 mg.

The peaks at 34.46 and 32.12 ppm in TNOAP can be assigned to the C₂ and C₃ carbons linked to the C₁ carbon that is directly attached to nitrogen of amine group. The peak at 21.47 ppm in TNPAP can be assigned to the carbon of a methylene (-CH₂-) group. The peaks at 29.93, 28.37 and 24.49 ppm in TNOAP can be assigned to the carbons of methylene (-CH₂-) groups. Peaks at 12.30 and 14.98 ppm in TNPAP and TNOAP can be attributed to the terminal -CH₃ group of amine molecules.^{13,28}

Based on the abovementioned characterization, we have proposed the following scheme for titanium aminophosphates synthesis and the basic structure of the catalysts. This is a tetrafunctional catalyst due to the presence of titanium ions (redox, Lewis acid), amines (Lewis base) and exchangeable proton (Bronsted acid) sites. As the reaction is carried out in solvent free condition, there is no waste from the synthesis of the catalyst (100% yield). Therefore, all the input titanium, amine and phosphorous are present in the basic structure. The presence of solid acid sites are deduced from the proposed structure, which is confirmed by the NaCl ion exchange experiment.

The catalytic degradation of crystal violet (CV) dye by hydrogen peroxide over TNPAP, TNOAP and TNDDAP was investigated at room temperature. The percentage degradation of CV was evaluated by measuring the decrease in absorbance of the CV solution with respect to time in the presence of hydrogen peroxide. The visible absorption maximum of CV was found to be 580 nm and all the degradation studies were carried out at this wavelength. It is observed that absorbance of CV decreases exponentially and tends to reach a saturation value after about 165 min. During the degradation of CV, the CV molecules get

Table 2 Effect of hydrogen peroxide concentration on the degradation of crystal violet^a

[H ₂ O ₂] × 10 ⁴ M	% degradation		
	TNPAP	TNOAP	TNDDAP
0.1	51.8	38.9	41.7
0.2	67.2	54.1	47.9
0.5	78.2	65.2	70.4
0.75	81.5	76.6	72.3
0.100	91.4	87.1	85.2
0.150	90.8	85.2	83.7
0.200	89.7	83.7	81.2

^a [CV] = 8.0 × 10⁻⁴ M, pH = 5.1, catalyst dosage = 150 mg.

Table 3 Effect of catalyst dosage on the degradation of crystal violet^a

Catalyst dosage (mg)	% degradation		
	TNPAP	TNOAP	TNDDAP
0	17.9	17.9	17.9
25	40.9	41.7	39.8
50	45.5	48.2	46.1
75	58.7	54.3	52.6
100	72.9	67.4	71.8
150	91.3	81.8	82.7
175	89.2	78.9	80.1
200	87.8	76.1	79.1

^a [CV] = 8.0 × 10⁻⁴ M, [H₂O₂] = 1.0 × 10⁻³ M, pH = 5.1.

adsorbed on the surface of the titanium aminophosphates. Thus adsorbed CV molecules react with the peroxy radicals generated from the reaction of hydrogen peroxide with titanium and get converted to a colorless benzenoid form of CV. This undergoes further degradation by repeated attack of the peroxy radicals.

pH plays a very important role in the degradation of dyes because it affects both the surface charge of the catalyst and the stability of dyes. The effect of pH on the degradation of CV has been studied by varying it in the range from 2.7 to 5.1 in the presence of TNPAP, TNOAP and TNDDAP catalysts by taking the hydrogen peroxide concentration as 1.0 × 10⁻³ M, CV concentration of 8.0 × 10⁻⁴ M and catalyst dosage of 150 mg. For all the titanium aminophosphate catalysts studied, the percentage degradation was found to increase with the increase in pH of the medium from 2.7 to 5.1. The results indicate that the degradation is significantly influenced by the pH of the solution. Among the titanium aminophosphate catalysts used for CV degradation, TNPAP is found to be the most efficient for the degradation of CV under the experimental conditions. The percentage of degradation increased from 64.1 at pH 2.7 to a maximum of 91.4 at pH 5.1 in 165 min in the presence of the TNPAP catalyst (Table 1). In basic medium, hydrolysis of CV occurs and therefore our studies are restricted to the acidic pH range. Increase in degradation of CV with increase in pH is due to higher adsorption of the cationic dye on the catalyst surface. As pH increases, interactions between dye molecules with surface hydroxyl groups of titanium aminophosphates increase due to changes in the electrostatic forces. Further studies on the degradation were carried out at pH 5.1.

H₂O₂ forms OH radicals, which interact with dye molecules and cause their degradation. The effect of varying the

Table 4 Effect of crystal violet concentration on the degradation of crystal violet^a

S. No	[CV] × 10 ⁻⁴ M	% degradation
1	2.0	91.2
2	4.0	91.0
3	6.0	91.1
4	8.0	91.3

^a [H₂O₂] = 1.0 × 10⁻³ M, pH = 5.1, TNPAP = 150 mg.

Table 5 Comparison of effect of titanium aminophosphate catalysts on degradation of CV^a

S. No	Catalysts	% degradation
1	TNPAP	91.4
2	TNOAP	87.1
3	TNDDAP	85.2

^a $[CV] = 8.0 \times 10^{-4}$ M, $[H_2O_2] = 1.0 \times 10^{-3}$ M, pH = 5.1, catalyst dosage = 150 mg.

Table 6 Reusability of TNPAP towards the degradation of crystal violet^a

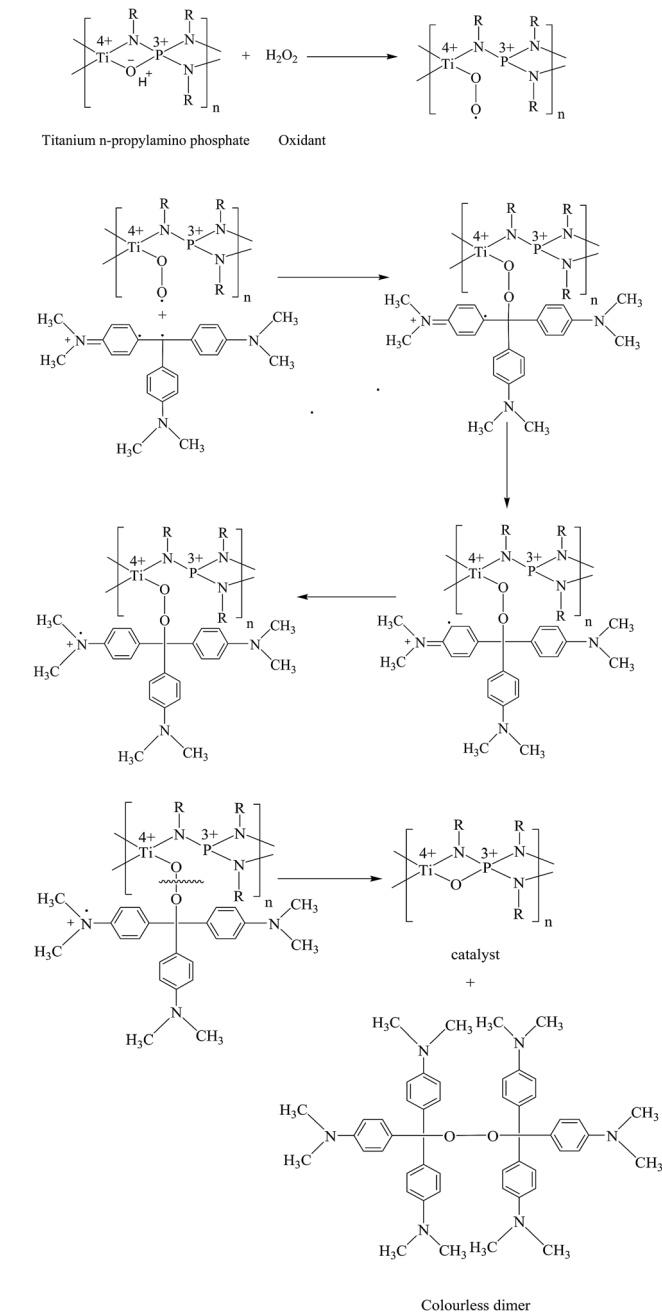
Catalyst	Fresh	Recycled 1	Recycled 2	Recycled 3	Recycled 4
% degradation	91.3	90.8	89.7	89.5	89.0

^a $[CV] = 8.0 \times 10^{-4}$ M, $[H_2O_2] = 1.0 \times 10^{-3}$ M, pH = 5.1, TNPAP = 150 mg.

concentration of hydrogen peroxide on the degradation of CV has been studied by varying the concentration of hydrogen peroxide in the range from 1.0×10^{-3} M to 2.0×10^{-3} M at pH 5.1 with a catalyst dosage of 150 mg. The extent of degradation was found to increase with an increase in hydrogen peroxide concentration until 1.0×10^{-3} M (Table 2). This can be ascribed to the increased number of OH radicals at higher concentrations of hydrogen peroxide that induces the reaction to proceed faster. Further increases in the concentration of hydrogen peroxide have little effect on the percentage degradation. After a particular concentration of hydrogen peroxide, the surface of the catalyst is saturated with OH radicals and it may form OH radical ions, which would not influence the degradation. This is due to the well-known hydroxyl radical scavenging effect at higher concentrations of hydrogen peroxide.²⁹ Therefore, 1.0×10^{-3} M of hydrogen peroxide is taken as optimum concentration for the degradation of CV.

The effect of catalyst dosage on the degradation of CV has been studied by varying the amount of catalyst in the range of 25–200 mg at pH 5.1 by keeping concentration of H_2O_2 at 1.0×10^{-3} M and CV concentration at 8.0×10^{-4} M. With increases in catalyst dosage from 25 mg to 150 mg, there is an increase in CV degradation from 40.9% to 91.3% in 165 min in the case of TNPAP (Table 3). Further increase in the amount of catalyst does not have much influence on the degradation of CV. As the amount of catalyst increases, more dye molecules get adsorbed on to the surface of the catalyst due to the increased number of active sites. Once all the dye gets adsorbed, further increase in the amount of catalyst has negligible effect on the extent of degradation. Therefore, 150 mg of catalyst is chosen as the optimum amount for degradation of CV under the experimental conditions.

The effect of varying the initial concentration of CV on its degradation in the presence of TNPAP has been studied under the optimum conditions of pH 5.1, $[H_2O_2] = 1.0 \times 10^{-3}$ M. The catalyst dosage was fixed as 150 mg. The results indicate that increasing CV concentration in the range 2.0×10^{-4} M to 8.0×10^{-4} M has no significant effect on the percentage of its

**Fig. 4** A plausible reaction mechanism of catalytic crystal violet dye degradation using titanium aminophosphates.

degradation (Table 4). This may be attributed to the saturation of catalyst surface with CV molecules at these concentrations. 8.0×10^{-4} M of CV has been chosen for all the studies on the degradation of CV such that the absorbance measurements are in a suitable range for the experiments.

The effect of titanium aminophosphate catalysts on the degradation of crystal violet dye has been compared under optimum conditions and the results are shown in Table 5. Among the three catalysts studied, TNPAP showed relatively higher catalytic activity than TNOAP and TNDDAP.

To explore the applicability of this method for crystal violet degradation in industrial wastewaters, the recyclability of the catalyst has been investigated under the optimum conditions of pH 5.1, catalyst dosage of 150 mg, $[H_2O_2] = 1.0 \times 10^{-3}$ M and $[CV] = 8.0 \times 10^{-4}$ M in the presence of TNPAP, the most efficient among the catalysts studied. Studies on the reusability of catalyst were carried out after the maximum degradation had been reached. The contents were centrifuged to recover the catalyst. It was washed with water followed by ethanol, dried and reused under the optimum experimental conditions. It is observed that the percentage degradation of CV remains nearly same even after five successive runs (Table 6). This confirms that the activity of TNPAP is retained after repeated use. These studies also reveal that there is no leaching of metal ions from the framework of the catalytic material even after several washings and usage.

Hydrogen peroxide reacts with the titanium atom of titanium aminophosphate and is converted to the titanium hydroperoxide radical (Fig. 4). Formation of this radical is confirmed by the presence of a yellow coloured solution. This titanium hydroperoxide radical is labile and inserts oxygen to the triphenyl substituted carbon of crystal violet. Therefore, conversion of the phenyl form to the quinone form occurs. This leads to changes in the colour. This quinone form is less stable and is converted to various fragments in the presence of hydrogen peroxide.

Conclusions

Titanium aminophosphates are prepared by using titanium tetraisopropoxide, orthophosphoric acid and aliphatic amines. The synthesized TNPAP, TNOAP and TNDDAP aminophosphates were characterized by various physicochemical techniques. Powder XRD spectra of titanium aminophosphates suggests the presence of a $-Ti-O-$ phase. The percentage of titanium incorporated into the frameworks of titanium aminophosphates has been confirmed from EDAX analysis. The infrared and Raman spectra infers the presence of peaks due to vibrational bands of Ti-O, P-O and Ti-O-P linkages. The UV-Vis diffuse reflectance spectra reveal the presence of tetrahedral coordination of Ti in the framework. The XPS spectra suggest the presence of $-O-Ti-N-$ or $-Ti-N-O-$ framework in TNPAP. The ^{31}P MASNMR spectra of titanium aminophosphates indicate the presence of tetrahedrally coordinated phosphorous in the framework. The catalytic effect of TNPAP, TNOAP and TNDDAP has been studied for the degradation of crystal violet. TNPAP has been found to be more efficient for the degradation of crystal violet, indicating the specificity of this catalyst. The optimum conditions required for the efficient degradation of crystal violet have been established as pH = 5.1, $[H_2O_2] = 1.0 \times 10^{-3}$ M, $[CV] = 8.0 \times 10^{-4}$ M and TNPAP catalyst dosage of 150 mg. About 91% of the crystal violet dye has been degraded by TNPAP in 165 min. These catalysts exhibited good reusability over five successive cycles. They have the potential to be used as economical catalysts for dye degradation of industrial wastewaters.

Acknowledgements

The authors A. R., A. A. K., S. C. and S. S are thankful to the MHRD, New Delhi for a fellowship.

References

- 1 P. C. Vandevivere, R. Bianchi and W. Verstraete, *J. Chem. Technol. Biotechnol.*, 1998, **72**, 289.
- 2 D. Karadag, S. Tok, E. Akgul, K. Ulucan, H. Evden and M. A. Kaya, *Ind. Eng. Chem. Res.*, 2006, **45**, 3969.
- 3 D. L. Ma, M. H. T. Kwan, D. S. H. Chan, P. Lee, H. Yang, V. P. Y. Ma, L. P. Bai, Z. H. Jiang and C. H. Leung, *Analyst*, 2011, **136**, 2692.
- 4 S. Pattapu, S. Saha, S. Jana, A. Pal and J. Eng, *International Conference on Composite/Nano Engineering (ICCE-16)*, Sun Light Publishing, Kumming, CHN, 2008.
- 5 S. K. Samantaray, T. Mishra and K. M. Parida, *J. Mol. Catal. A: Chem.*, 2000, **156**, 267.
- 6 S. K. Samantaray and K. M. Parida, *J. Mol. Catal. A: Chem.*, 2001, **176**, 151.
- 7 A. K. Cheetham, G. Ferey and T. Loiseau, *Angew. Chem., Int. Ed. Engl.*, 1999, **38**, 3268.
- 8 C. Berlini, M. Guidotti, G. Moretti, R. Psaro and N. Ravasio, *Catal. Today*, 2000, **60**, 219.
- 9 K. Khosravi, M. E. Hoque, B. Dimock, H. Hintelmann and C. D. Metcalfe, *Anal. Chim. Acta*, 2012, **713**, 86.
- 10 D. M. Antonelli and J. Y. Ying, *Angew. Chem., Int. Ed. Engl.*, 1995, **34**, 2014.
- 11 A. R. Khataee and M. B. Kasiri, *J. Mol. Catal. A: Chem.*, 2010, **328**, 8.
- 12 M. Nagao and Y. Suda, *Langmuir*, 1989, **5**, 42.
- 13 L. Zhang, J. Xu, G. Hou, H. Tang and F. Deng, *J. Colloid Interface Sci.*, 2007, **311**, 38.
- 14 K. M. Parida, M. Acharya, S. K. Samantaray and T. Mishra, *J. Colloid Interface Sci.*, 1999, **217**, 388.
- 15 S. F. Lincoln and D. R. Stranks, *Aust. J. Chem.*, 1968, **21**, 37.
- 16 X. A. Zhao, C. W. Ong, Y. C. Tsang, Y. W. Wong, P. W. Chan and C. L. Choy, *Appl. Phys. Lett.*, 1995, **66**, 2652.
- 17 S. Sakka, F. Miyaji and K. Fukumi, *J. Non-Cryst. Solids*, 1989, **112**, 64.
- 18 N. G. Chernorukov, I. A. Korshunov and M. I. Zhuk, *Russ. J. Inorg. Chem.*, 1982, **27**, 1728.
- 19 A. Nilchi, M. G. Maragheh, A. Khanchi, M. A. Farajzadeh and A. A. Aghaei, *J. Radioanal. Nucl. Chem.*, 2004, **261**, 393.
- 20 B. B. Sahu and K. Parida, *J. Colloid Interface Sci.*, 2002, **248**, 221.
- 21 C. Schmutz, P. Barboux, F. Ribot, F. Taulelle, M. Verdaguer and C. Fernandez-Lorenzo, *J. Non-Cryst. Solids*, 1994, **170**, 250.
- 22 X. Gao and I. E. Wachs, *Catal. Today*, 1999, **51**, 233.
- 23 L. A. Farrow and E. M. Vogel, *J. Non-Cryst. Solids*, 1992, **143**, 59.
- 24 H.-F. Yu and S.-T. Yang, *J. Alloys Compd.*, 2010, **492**, 695.
- 25 K. M. Parida and N. Sahu, *J. Mol. Catal. A: Chem.*, 2008, **287**, 151.

26 C. Di Valentin, E. Finazzi, G. Pacchioni, A. Selloni, S. Livraghi, M. C. Paganini and E. Giamello, *Chem. Phys.*, 2007, **339**, 44.

27 E. Jaimez, A. Bortun, G. B. Hix, J. R. Garcia, J. Rodriguez and R. C. T. Slade, *J. Chem. Soc., Dalton Trans.*, 1996, 2285.

28 A. Hayashi, H. Nakayama and M. Tsuhako, *Solid State Sci.*, 2009, **11**, 1007.

29 F. A. Alshamsi, A. S. Albadwawi, M. M. Alnuaimi, M. A. Rauf and S. S. Ashraf, *Dyes Pigm.*, 2007, **74**, 283.